IOPscience iopscience.iop.org

Home Search Collections Journals About Contact us My IOPscience

Amorphisation and recrystallisation study of lithium intercalation into TiO_2 nano-architecture.

This content has been downloaded from IOPscience. Please scroll down to see the full text.

2017 IOP Conf. Ser.: Mater. Sci. Eng. 169 012020

(http://iopscience.iop.org/1757-899X/169/1/012020)

View the table of contents for this issue, or go to the journal homepage for more

Download details:

IP Address: 129.12.60.182
This content was downloaded on 20/04/2017 at 12:00

Please note that terms and conditions apply.

You may also be interested in:

Recovery and recrystallisation in mechanically alloyed and annealed, legacy, FeCrAlY ODS alloy precursor powders
K Dawson, A Rao, G J Tatlock et al.

Template synthesis and characterization ofWO3/TiO2 composite nanotubes
Lifang Cheng, Xingtang Zhang, Bin Liu et al.

The prospects of phosphorene as an anode material for high-performance lithium-ion battery: a fundamental study
Congyan Zhang, Ming Yu, George Anderson et al.

Facile hydrothermal synthesis of porous TiO2 nanowire electrodes with high-rate capabilityfor Li ion batteries
Hyun-Woo Shim, Duk Kyu Lee, In-Sun Cho et al.

Amorphisation and recrystallisation study of lithium intercalation into TiO_2 nano-architecture.

M G Matshaba[1], D C Sayle[2], T X T Sayle[1, 2] and P E Ngoepe[1]

[1]Materials Modelling Centre, School of Physical and Mineral Sciences, University of Limpopo, Private Bag X 1106, Sovenga, 0727, South Africa.
[2]School of Physical Sciences, University of Kent, Canterbury, Kent, CT2 7NZ, United Kingdom.

malili.matshaba@ul.ac.za

Abstract.Titanium dioxide is playing an increasingly significant role in easing environmental and energy concerns. Its rich variety of polymorphic crystal structures has facilitated a wide range of applications such as photo-catalysis, photo-splitting of water, photoelectrochromic devices, insulators in metal oxide, semiconductors devices, dye sensitized solar cells (DSSCs) (energy conversions), rechargeable lithium batteries (electrochemical storage). The complex structural aspects in nano TiO_2, are elucidated by microscopic visualization and quantification of the microstructure for electrode materials, since cell performance and various aging mechanisms depend strongly on the appearance and changes in the microstructure. Recent studies on MnO_2 have demonstrated that amorphisation and recrystallisation simulation method can adequately generate various nanostructures, for Li-ion battery compounds. The method was also previously employed to produce nano-TiO_2. In the current study, the approach is used to study lithiated nanoporous structure for TiO_2 which have been extensively studied experimentally, as mentioned above. Molecular graphic images showing microstructural features, including voids and channels have accommodated lithium's during lithiation and delithiation. Preliminary lithiation of TiO_2 will be considered.

1. Introduction

Titanium dioxide is an oxide that is chemically stable, inexpensive, nontoxic and photocatalytic [1]. It has many applications including electrochemical storage for rechargeable lithium ion batteries (LIBs) [2, 3]. Much as the TiO_2 nanoparticles introduce good electrochemical performance of anodes for LIB they also have limitations. It is well known that nanoparticles possess high surface energy compared with the bulk counterpart and incline to aggregate either during synthesis or galvanostatic cycling. The aggregation of nanoparticles decreases the surface area and increases the difficulty for electrolyte solution diffusion within aggregates reaching the surface of particles; it results in the reduction of the total storage energy. Consequently, a better way to avoid this situation is to prepare nanoporous TiO_2 [4]. Nanoporous TiO_2 have been studied by several authors [5, 6, 7, 8] and the micrometre-sized mesoporous materials have characteristic grains as well as pores nearly in the same scale. Electrodes of mesoporous materials for lithium batteries have short transport lengths for Li^+ ions due to their nano-sized grains (10–20 nm), and easy access for electrolytes due to their nanopores (5–10nm). Such mesoporous materials have high packing densities unlike nanopowders, nanowires, nanorods and nanotubes. Despite such advantages, electronic conduction over micrometer-sized particles limits the rate performance of mesoporous materials.

Content from this work may be used under the terms of the Creative Commons Attribution 3.0 licence. Any further distribution of this work must maintain attribution to the author(s) and the title of the work, journal citation and DOI.
Published under licence by IOP Publishing Ltd

Ren et al. (2010) [9] synthesized an ordered 3D mesoporous anatase using a hard template and investigated lithium intercalation. The structural changes are similar to those observed for nanoparticles, with continuous Li insertion into tetragonal anatase up to $Li_{0.05}TiO_2$, then a two-phase process between anatase and orthorhombic $Li_{0.45}TiO_2$ followed by continuous insertion into the orthorhombic phase up to $Li_{0.96}TiO_2$.
In this work we simulate lithiated nanoporous of TiO_2 to investigate the storage capacity as an anode material inside a LIB. We explore microstructural graphics of our system to see Li ions that move and reside within the nanoporous material. Validation of our model will be accomplished by calculating X-Ray Diffraction patterns (XRDs) which will be compared with the experimental data.

2. Methodology

Potential model and simulation code:
The Calculations are based on the Born model of ionic solids, where Ti^{4+}, Ti^{3+}, Li^{+} and O^{2-} ions interact via long-range Coulombic and short range parameterised interactions. A charge is assigned to each atom and the long range attractive interactions between charged ions is balanced by short range repulsive interactions. Model parameters that are used to characterize Li-TiO_2 are specified in table 1 and are taken from Sayle [10] and Sayle [11].
All the molecular dynamics simulations were performed using DL_POLY code [12]. The user manual provides comprehensive analytical descriptions and discussion of the molecular dynamics simulations, force fields, boundary conditions, algorithms and parallelisation methods used in these simulations.

Table 1. Potential parameters describing the short-range potential terms between the component ion species of $LiTiO_2$ used for lithiated TiO_2

interaction (ij)	A_{ij} (Å)	ρ_{ij} (Å)	C_{ij} (eV.Å6)	charge
Ti^{3+}-O^{2-}	18645.84	0.195	22.0	
Ti^{4+}-O^{2-}	16957.53	0.194	12.59	
Li^{+}-O^{2-}	426.48	0.300	0.00	
Ti^{3+}-Ti^{4+}	28707.21	0.156	16.0	
Ti^{3+}-Ti^{3+}	33883.92	0.156	16.0	1.65
Li^{+}-Li^{+}	270000.00	0.143	0.0	0.55
Ti^{4+}-Ti^{4+}	31120.20	0.156	5.25	2.196
O^{2-}-O^{2-}	11782.76	0.234	30.22	-1.098

Generating atomic model
The atomic model for nanoporous architecture was generated using molten TiO_2 nanoparticle precursor. In particular, a particle of TiO_2 comprising 15 972 atoms (5324 titanium and 10648 oxygen atoms), was

cut from the parent bulk material. The nanoparticle was then melted by heating to 6000 K, which is above the melting point for TiO_2, under MD simulation. The molten nanoparticle was then used as the 'building-block' to generate the nanoporous architectures. To capture the (cubic) symmetry of the nanoporous architecture, a simulation cell with cubic symmetry was constructed and a nanoparticle of TiO_2 was positioned at lattice points associated with the primitive cubic Bravais lattice. The size of the simulation cell was then reduced in all three dimensions to enable the nanoparticle to agglomerate in all three spacial directions. NVT simulation was then performed at 2000 K for 3.5 ns to facilitate crystallisation. Periodic boundary conditions were used to replicate the structure infinitely in three dimensions. The low-temperature structural model was then generated by cooling the system to 0 K under NVT MD simulation until the configurational energy converged. The same procedure was performed to create nano-architectures of TiO_2 [13].
Then Li-TiO_2 was generated by randomly inserting 100 Li ions in the amorphous nanoporous TiO_2 at the specific coordinates. Charge compensation in the nanoporous is achieved by changing the titanium (4+ oxidation state) closest to the lithium cation into the Jahn-Teller active titanium (3+ oxidation state). This process is repeated for all the lithium ions inserted in the nanoporous. Amorphous nanoporous structure of Li-TiO_2 is depicted in figure 1 below. Oxygen atoms are red coloured, Titanium are grey and lithium ions are represented by yellow balls.

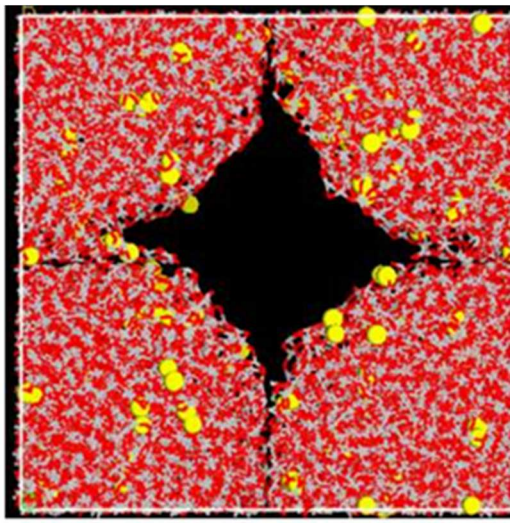

Figure 1. Snapshot of lithiated amorphous nanoporous structure of TiO_2 with 100 Li ions.

3. Results

We performed a molecular dynamics simulation using the NVT ensemble, at a temperature of 2000 K for 700000 steps with a time step of 0.005 ps, in order to recrystallise a lithiated nanoporous of TiO_2. A plot of configuration energy as a function of time is shown in figure 3, indicating that the nanoporous is fully recrystallised since the configuration energy is constant at the energy of -2.04x 10^5 eV. The sudden decrease in energy from 0 to 0.5 ns indicates the transition from amorphous to a crystalline phase.

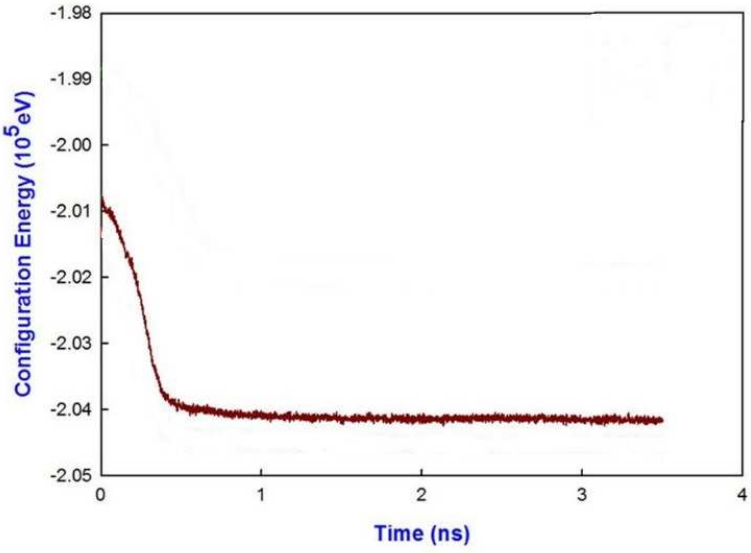

Figure 2. Configuration energy as a function of time for nanoporous TiO_2.

Superimposed radial distribution functions (RDFs) of the amorphous and recrystallised nanoporous structure of Li-TiO_2 are illustrated in figure 3 below. They clearly indicate that our system is recrystallised since the RDFs of recrystallised material shows some sharp picks than the amorphous structure.

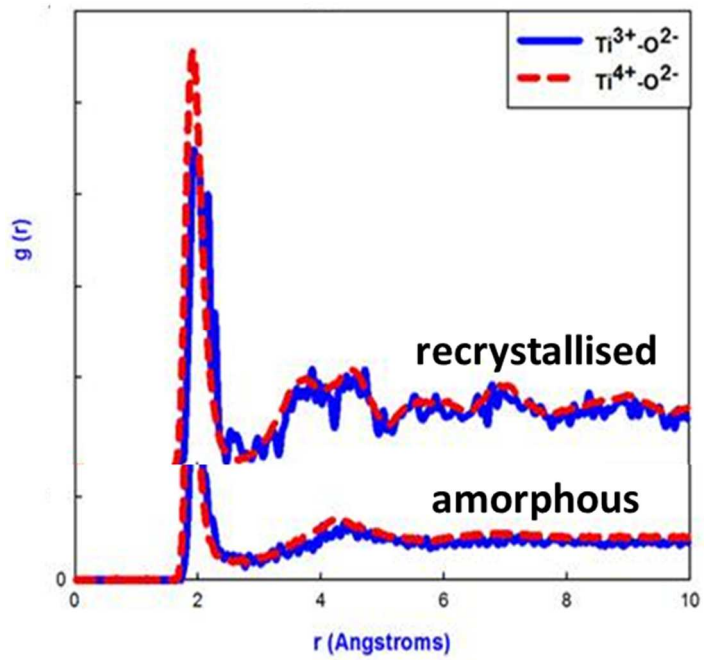

Figure 3. RDFs of lithiated nanoporous of TiO_2 before and after recrystallisation.

The recrystallised lithiated nanoporous of TiO_2 which is depicted in figure 4 was cooled by running molecular dynamics (MD) simulation for 500 ps at 1500 K, followed by 250 ps at 1000 K, 250 ps at 500 K, and lastly 500 ps at 0 K. A similar process was employed in generating the MnO_2 nanosphere [14]. Cooled nanoporous structure of Li-TiO_2 is illustrated in figure 4 and we observe more vacancies next to the channel. Lithium atoms are located closer to the inner edge of the channel in the cooled nanoporous

structure of Li-TiO_2 than in the uncooled one; crystalline patterns are more distinct as compared with the ones at higher temperatures.

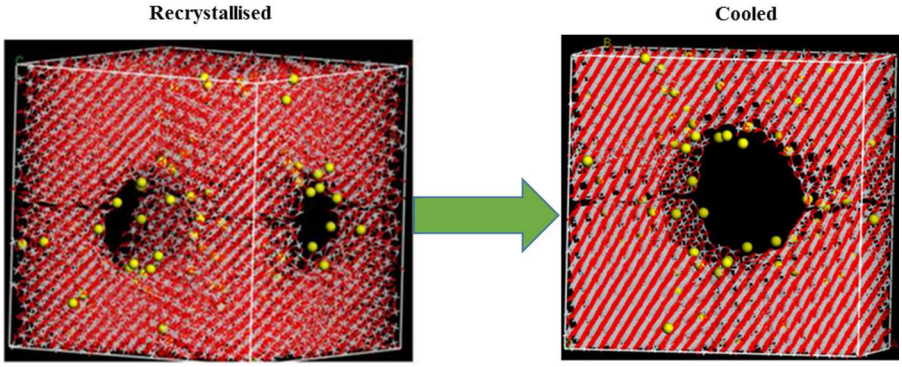

Figure 4. Recrystallised and cooled lithiated nanoporous of TiO_2.

Created microstructure of lithiated nanoporous structure of TiO_2 is shown in figure 5 below. Yellow balls are Li atoms, blue octahedral is the upper layer of Ti^{4+} and the white adjacent correspond to the lower layer of Ti^{4+}. We observe more microstructural characteristics in the nanoporous: rutile, brookite, vacancies, Li's in tunnels, stacking defect, micro-twinning and Li atoms in vacancies. Rutile phase is depicted by the straight tunnels and the brookite phase is characterised by zigzag tunnels. For a nanoporous to be a good candidate of anode material it has to store more Li atoms and be able to have pathways so that it can allow Li atoms to pass through. With Li atoms occupying the lower layer and vacancies it indicate that the nanoporous of TiO_2 can store Li atoms. The material also shows that it can be able to transport Li atoms since it has a clear tunnels and some Li atoms can pass through vacancies.

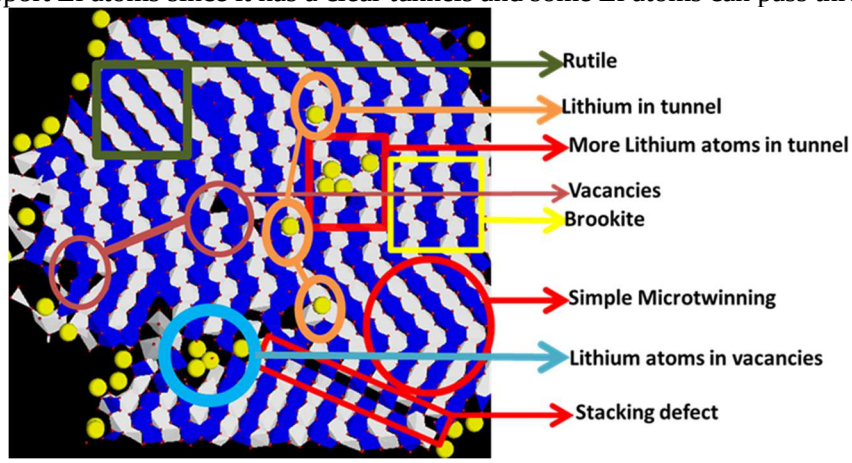

Figure 5. Microstructure of cooled lithiated nanoporous of TiO_2.

On superimposing XRD patterns of the experimental brookite [15], TiO_2: α-PbO_2, rutile polymorphs and the simulated TiO_2 nanosphere, corresponding peaks can be deduced. XRD's are depicted in figure 6 below. At 27, 33 and 37 ° there are sharp peaks that correspond well with the brookite and TiO_2: α-PbO_2 structure, whilst at 42 ° only the simulated, brookite and TiO_2: α-PbO_2 peaks are aligned. The simulated XRD pattern at 50 ° has a smooth curve which tally well with the rutile structure. The peaks at 37 and 57 ° correspond with all polymorphs and the one at 67 ° accords more reasonably with the rutile and TiO_2: α-PbO_2 structures.

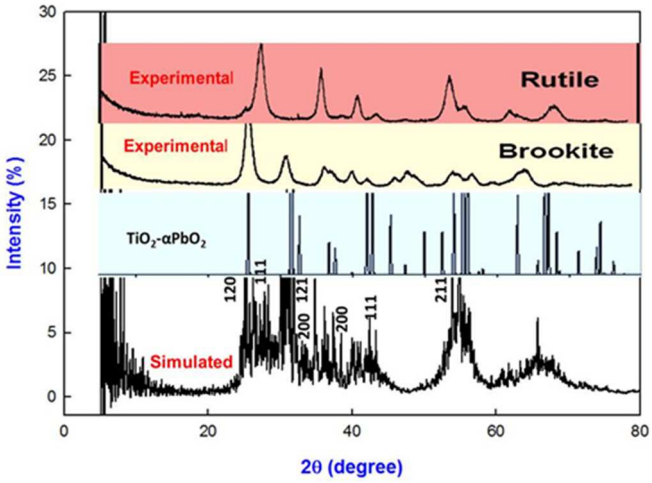

Figure 6. A comparison of simulated TiO_2 nanoporous, calculated TiO_2:α-PbO_2 and experimental[15] XRDs.

4. Conclusion

Molecular dynamics simulation has been used successfully to generate atomistic model of nanoporous Li-TiO_2. The nanoporous of Li-TiO_2 was fully recrystallised and cooled to a 0 K. The recrystallised material was confirmed by the RDFs, which depict sharp picks. Microstructure reveal that the nanoporous of TiO_2 can act as a good anode material since it can store and transport Li atoms during charging and discharging of a battery. XRDs depict the presence of rutile and brookite phases as compared with the experimental data.

Acknowledgements

Calculations were performed at Materials Modelling Centre (MMC), University of Limpopo. This work is supported by Department of Science and Technology, National Research Foundation, Pretoria, the Department of Science and Technology HySA Lithium Ion Batteries and Supercapacitors Project, Pretoria and the Centre for High Performance Computing (CHPC) in South Africa.

References

[1] Liang Y, Gan S, Chambers S A and Altman E I, 2001 *Phys. Rev. B.* **63** 235402-1.
[2] Liu B and Aydil E S, 2009 *J. Am. Chem. Soc.* **131** (11) 3985.
[3] Fujishima A and Honda K, 1972 *Nature* **238** 37.
[4] Hwang K-J, Cho D W, Lee J-W and Im C, 2012 *New J. Chem.* **36** 2094.
[5] Zhou H S, Li D L, Hibino M and Honma I, 2005 *Angew. Chem. Int. Edit.* **44** 797.
[6] Moriguchi I, Hidaka R, Yamada H, Kudo T, Murakami H and Nakashima N, 2006 *Adv. Mater.* **18** 69.
[7] Guo Y G, Hu Y S, Sigle W and Maier J, 2007 *Adv. Mater.* **19** 2087.
[8] Wang Z Y, Liu S Z, Chen G and Xia D G, 2007 *Electrochem. Solid Sate Lett.* **10** (3) A77.
[9] Ren Y, Hardwick L J and Bruce P G, 2010 *Angew. Chem. Int. Ed.* **49** 2570.
[10] Sayle D C and Sayle T X T, 2007 *J. Comput. Theor. Nanosci.* **4** 299.
[11] Sayle T X T, Ngoepe P E and Sayle D C, 2009 *ACS Nano* **3** (10) 3308.
[12] Smith W and Forster T R, 1996. http://www.dl.ac.uk/TCSC/Software/DLPOLY.
[13] Matshaba M G, Sayle D C, Sayle T X T and Ngoepe P E, 2016 J. Phy. Chem. C 120 (26) 14001.
[14] Sayle T X T, Catlow C R A, Maphanga R R, Ngoepe P E and Sayle D C, 2005 *J. Am. Chem. Soc.* **127** 12828.
[15] Dambournet D Belharouak I and Amine K, 2009 *Electrochem. Soc.* **215**, No.1.